Complex terrain wind resource estimation with the wind-atlas method: Prediction errors using linearized and nonlinear CFD micro-scale models

Troen, Ib; Bechmann, Andreas; Kelly, Mark C.; Sørensen, Niels N.; Réthoré, Pierre-Elouan; Cavar, Dalibor; Ejsing Jørgensen, Hans

Published in:
Proceedings of EWEA 2014

Publication date:
2014

Document Version
Publisher's PDF, also known as Version of record

Complex terrain wind resource estimation with the wind-atlas method: Prediction errors using linearized and nonlinear CFD micro-scale models.

Ib Troen, Andreas Bechmann, Mark C. Kelly, Niels N. Sørensen, Pierre-Elouan Réthoré, Dalibor Cavar, Hans E. Jørgensen

Wind Energy, DTU, Denmark

ibtr@dtu.dk

Abstract

Using the Wind Atlas methodology to predict the average wind speed at one location from measured climatological wind frequency distributions at another nearby location we analyse the relative prediction errors using a linearized flow model (IBZ) and a more physically correct fully non-linear 3D flow model (CFD) for a number of sites in very complex terrain (large terrain slopes). We first briefly describe the Wind Atlas methodology as implemented in WAsP and the specifics of the "classical" model setup and the new setup allowing the use of the CFD computation engine. We discuss some known shortcomings of the linear orographic flow model (BZ) and possible modifications that could be considered, including the established RIX method.

1 Wind Atlas methodology

The wind atlas methodology [2] was designed for horizontal and vertical extrapolation of mean wind conditions for use in wind power resource estimation. That is, if one has long term measured wind data (speed and direction) from some point (met mast location) at some height above ground, the method is used to estimate the wind conditions (wind speed frequency distributions per direction sector) at some other point of interest (hub height of wind turbine). The method assumes that winds in the points considered are governed by the same large- (meso-) scale wind forcing. In practice this means that the horizontal distance over which the method can be meaningfully applied depend on the scales of the overall climate and of the scales of flow modifications introduced by surface inhomogeneity (roughness differences, thermal differences, hills and mountains).

The methodology involves two distinct parts: The "Wind Atlas Analysis" in which the measured wind data are transformed using micro-scale models to estimate the local influences at the measuring point, subtracting these and using Rossby number similarity theory (" Geostrophic drag law") [5] to give a "Wind Atlas data set" , figure 1.

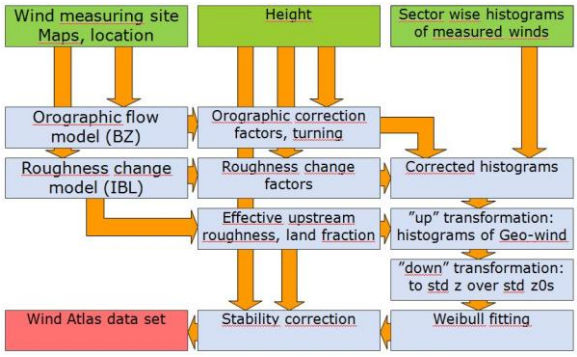

Figure 1: Wind Atlas Analysis, adapted from [2]. The user input is indicated in green, the internal machinery as light blue blocks and orange arrows, results in red.

The second part is the "Wind Atlas Application" in which the same micro-scale models are used to introduce the flow perturbations at the location

and height of interest (e.g. the real or prospective location and hub height of a Wind Turbine) (figure 2).

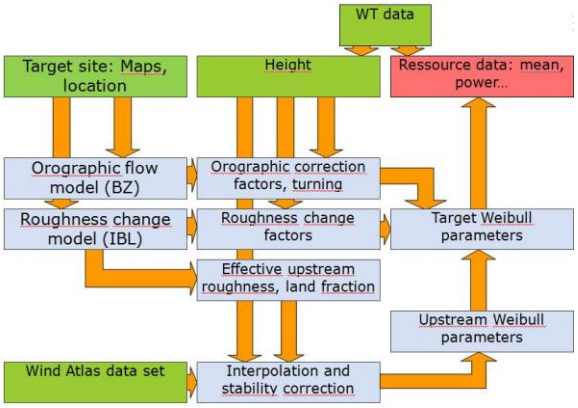

Figure 2: Wind Atlas Application, adapted from [2]

The "Wind Atlas Analysis and Application Program" (WAsP) contain these two parts with the built-in orographic flow model (BZ) [2, 6] and the simple "internal boundary layer" (IBL) model for surface roughness inhomogeneities [2, 7]. Recently the WAsP has been modified to allow these internal (essentially) linear models to be replaced by external models, e.g. nonlinear models based "Reynolds Averaged Navier-Stokes" (RANS) equations. Such models require considerable more computing resources than standard WAsP and therefore these model simulations must currently be run on a remote cluster, figs 3. The terrain maps are transferred via the web (the clouds in the figure) together with specification of the target area to the remote cluster where grid generation and the running of the Ellipsys model takes place. The results (flow perturbations relative to specified far upstream inflow logarithmic profile) are returned via the web as a "result volume" giving the calculated flow corrections per upstream wind direction in a regular horizontal grid and at several levels above the ground. Within WAsP the internal models are thus replaced with interpolation within the result volume.

The purpose of this paper is to compare the skill in making cross predictions in very complex terrain of the two WAsP configurations, which we will denote WAsP-IBZ for the "standard" version with the linear internal flow models, and WAsP-CFD for the configuration using the remote Ellipsys model.

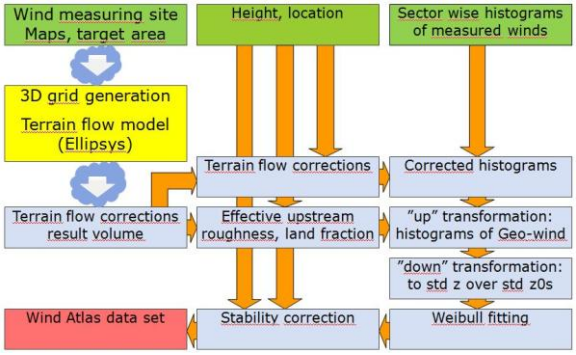

Figure 3: Wind Atlas Analysis using the Ellipsys RANS model, replacing part of the left blocks in figure 1. The corresponding Wind Atlas Application uses the same replacement of the two left column blocks (but in figure 2).

2 The BZ model

The linearized flow model in WAsP-IBZ [2,4] has been shown to compare well with other similar models for flow over hills [4,6] when applied to model flow over isolated hills.The linearized models tend to fail where full or partial/intermittent flow separation may occur e.g. in the lee of steep hills [8]. However, even in non-separated situations most linearized models (including BZ) neglect the effect on the pressure perturbation on the flow from the (assumed thin) disturbed layer near the surface by forcing the so-called "outer-layer" of irrotational flow with a boundary condition for the vertical velocity applied at the surface. The analyses in [9,10] show that more correctly the terrain forcing of the pressure field should be determined by the vertical velocities at some higher level h_m, which for idealized two dimensional sinusoidal orography can be estimated as:

$$h_m \sqrt{\log\left({}^{h_m}/_{z_0}\right)} = \frac{1}{4}\,\lambda\,,$$

where λ is the wavelength of the hills and z_0 the surface roughness. For typical values of interest this height can become several hundred meters.

At the same time, the pressure perturbation at a height z above the surface in the linear model is modeled like:

$$p(z) = p(0)\exp(-kz),$$

Where *k* is the wavenumber.Thus streamline slopes decay with height in the linear model possibly not at the correct rate. Separation is not modeled in the linear model (figure 4).

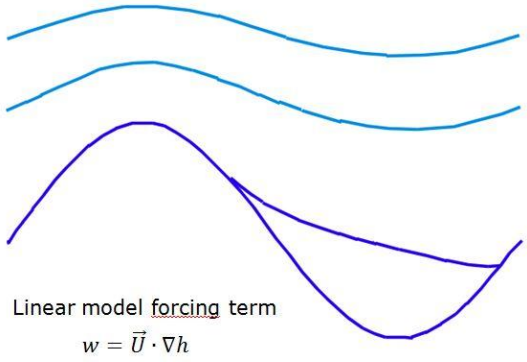

Figure 4: The linear BZ model uses the slope of the surface (dark blue sinus curve). The more correct forcing corresponds to the smaller slope of the light blue streamlines. In this case separation occurs and a separating streamline is indicated.

In general complex terrain estimation of h_m is difficult because of the many scales involved. For sinusoidal orography the analyses in [9,10,11], which are dealing with the estimation of the increased drag caused by the terrain relief (the so called "form-drag", which can be shown to be essentially proportional to the phase shift of the streamlines relative to the surface), show that this phase shift is quite small even in high profile terrain. This would suggest that a possible improvement of the skill of the linearized model could be obtained by reducing the surface slope. Here we attempt this by a simple "land-filling" method: simply adding "ground" upstream and downstream to result in a specified maximum slope value (the separation line in figure 4 illustrates this.

2.1 The "Ruggedness IndeX (RIX)"

In [3] a correction method to the WAsP model predictions in very steep terrain is described. It builds on some of the same general observations as sketched above, but instead of modifying the BZ model it consists of a correction to the full model cycle going from observed data at location A to predicted wind condition (mean wind speed u_m) at location B:

$$u_m(B) = u_{WAsP}(B) / \left(1 + c\left(RIX(B) - RIX(A)\right)\right)$$

The site RIX is determined as a sort of average area of high relief terrain as seen in a omndirectional site centered manner within a circle of a specified radius (figure 5).

The method involves the choice of the radius of the considered circle and the limit slope value. The method as standard requires calibration of the constant *c* in the above relation. The calibration requires the availability of several wind data sets from within the general area of interest [3]. In the validation below we will use a global calibration, since at most sites we have too few mast locations for a meaningful local calibration.

2.2 Orographic form drag

When the terrain is flat or with only very moderate slopes the surface drag is governed by the surface roughness (viscous drag). With substantial terrain relief (as in most of the case here with significant RIX values) the additional drag introduced by the pressure forces on the terrain slopes (form drag) can become much larger than the viscous drag [11]. In addition this drag force acts on the atmosphere in a deeper layer and not as a surface force like surface roughness [14]. The IBZ model does not include this drag. Since RIX is an indicator of steep slopes (and of BZ model deficiency [3], see also section 5) it may also be an indicator of higher form drag.

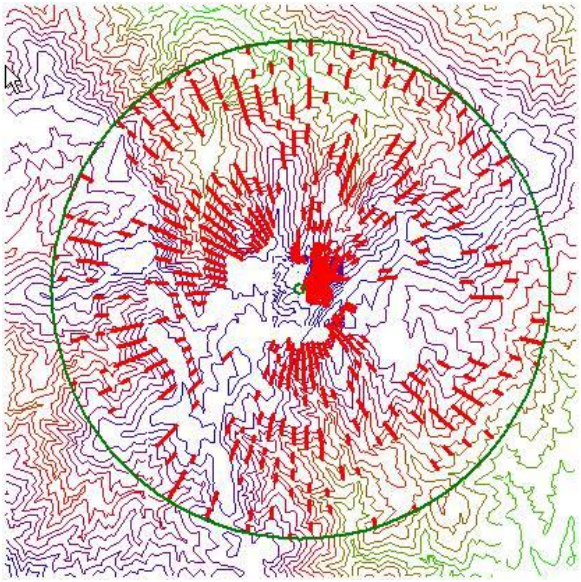

Figure 5: Illustration of the RIX determination in WAsP: A number of radial rays from the site out to a specified radius (default is 3.5km) is examined for the slope in the radial direction, where the absolute value exceeds a specified value (default is 0.3) that part of the ray is counted (indicated in red). The relative length of each ray defines a ray-RIX number and the site RIX is defined as the average of the ray-RIX values. Reproduced from [3].

If so, an improvement (replacing RIX with a less empirical method for the formdrag) could be based on including a (even crude) form drag formulation explicitly in the simple linear model setup (the parametrizations suggested in [10], [11] and [14] could be used for inspiration albeit being formulated for larger scales).

3 The Ellipsys model

The Ellipsys3D code [13, 15 and 16] is used in the WAsP-CFD configuration. As explained above the model including grid generation is done externally to WAsP with input maps and the resulting flow corrections communicated via web links. The EllipSys3D code is a multiblock finite volume discretization of the incompressible Reynolds Averaged Navier-Stokes (RANS) equations in general curvilinear coordinates.In WAsP-CFD configuration the model is setup for purely neutral atmospheric stability (as BZ), making it Reynolds number independent, meaning that flow perturbations will be independent of the inflow wind speed scale and only one simulation needs to be done per inflow direction.36 CFD simulations with different inflow directions are conducted for each WAsP-CFD result. Turbulence is modeled using two equation k-ε (turbulent energy and dissipation) closure [17]. The adaptation to the specific (automated) application used here will be detailed in an upcoming publication [12]. The model has been shown to well reproduce the Askervein experimental data [13] and was among the best performing RANS models in the Bolund model blind comparison (described in [1, 8]). As a fully dynamical model it does model highly disturbed flow situations including flow separation and should also model the form drag.

However, in its current and reasonably foreseeable configuration for WAsP-CFD, the inflow profiles are specified as function of the upstream surface roughness and not taking into account possible formdrag contributions. A development of simple formdrag model as discussed in the previous section could also help improve the CFD model setup.

For the below validation of WAsP-CFD we use as input the exact same maps, wind data and site specifications as for the linear WAsP-IBZ configurations. The results from the Ellipsys simulations are returned as mentioned above in the form of a 3D grid of flow corrections over a square “tile” of size 2km by 2km with 20m horizontal resolution. The actual computational area is of course much larger but the limit of the size of the result volume is intended to ensure that the quality of the results is quasi constant within the tile. Here we use only the minimum number of tiles: If two or more locations can fall within one tile that tile is used for these locations. When locations are further separated, tiles are used with the location at the tile center.

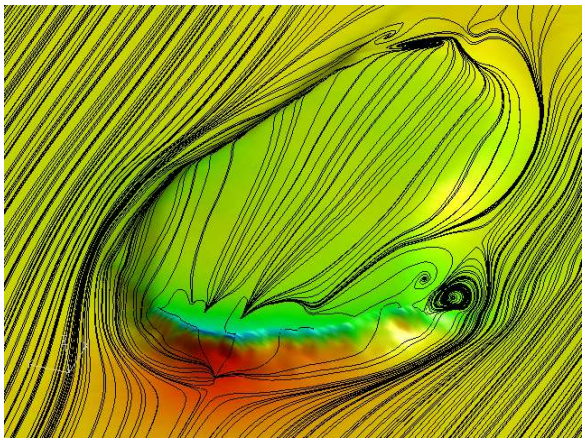

Figure 6: Surface streamlines from Ellipsys modeling of the flow over Bolund illustrating the models ability to produce flow separation upwind and downwind of steep slopes. Reproduced from [1].

4 Validation data

The validation is intended to document the skill of these model setups for use in real world wind resource estimation. We have used data from 9 sites with a total of 26 mast locations, most masts with several levels instrumented. The data was mainly provided by wind power developers, and the masts and sites were therefore chosen at or near potential wind energy installations. This means well exposed hills and ridges in general windy settings in complex terrain. The sites are located in Europe (5), Americas (2), and Southeast Asia/Australasia (2). The data and site descriptions are covered by Non-Disclosure-Agreements, so the individual cases cannot be discussed. We present a purely statistical analysis of the errors in cross predictions between wind observation locations based on the digitized maps, mast locations, anemometer/wind-vane heights and wind data (frequency distributions) provided to us. Most (6) sites were chosen by EMD international A/S among data held in their archives for which concurrent measured data could be extracted for several masts and covering at least a period of approximately one year, and for which the linear WAsP-IBZ was known to be beyond its “comfort-zone” because of very steep slopes and with the aim of testing the improvement offered by the WAsP-CFD configuration. We have included additional three also very complex sites including the Portuguese site used for development of the original RIX method [3].

The data from the 26 masts allow the selection of a total of 370 data pairs that can be used for finding the prediction errors of the mean wind speeds. The measuring heights vary from 10m (RIX site only) to 100m (one site). Most heights in the 40-80m range. Mast distances vary from approximately 1 km to 15km, with most distances a few km (overall average: 5km). See figure 13.

5 Prediction errors for the WAsP configurations

When considering the model prediction errors in complex terrain one should first realize the important difference between this situation and the more classical model validation (e.g. [4], [8]), where the inflow reference is generally well defined and undisturbed, and in addition one looks at single flow cases. Here we have several differences: We have in general to use input data, which are in the complex terrain and thus “disturbed” and predict at another “disturbed” site; we use climatological data that are truncated in sectors (here we use 12 sectors) and we predict over relatively large horizontal distances (km).

We select the (90) measurement pairs with anemometers ar equal height and divide in 4 height groups (10-20m, 30-40m, 50-60m and 80-100m) of roughly same size. For each we show the prediction errors in percent:

$$error = 100 \left| \frac{predicted - observed}{observed} \right|$$

(vertical axis in the plots) versus an arbitrary x-axis from 50-100pct with the errors for each configuration sorted in ascending order of the error. Thus in general the pair corresponding to the error at a given x value is different for each configuration. The plots (figure 8-11) show a measure of “confidence” or inversely “risk”,

selecting an “acceptable” error level (e.g. 10pct as indicated in the plots) one can see the pct of cases that fall below or above this limit.

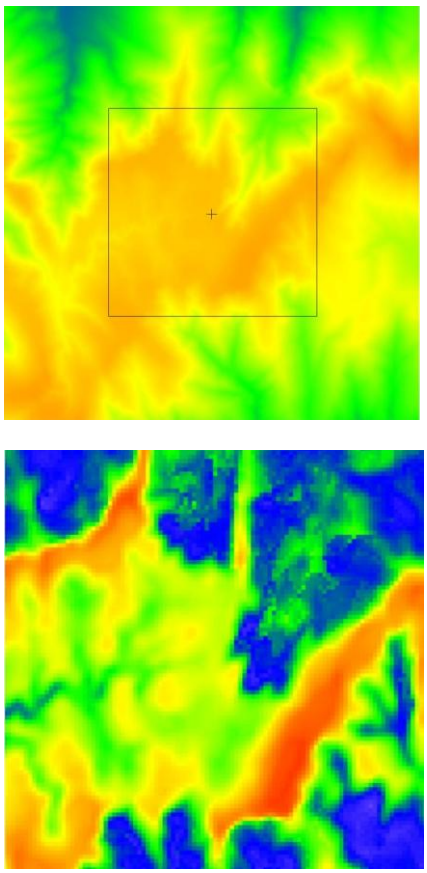

Figure 7: Illustration of validation site. The top frame is a 4 by 4 km square with the met mast indicated in the center. Below is the central 2 by 2 km tile from the CFD run with the predicted mean wind speed at 10m a.g.l. indicated in color (top, blue to orange approx 100m to 1000m, bottom (blue to red) approx a factor 7 in mean wind speed.

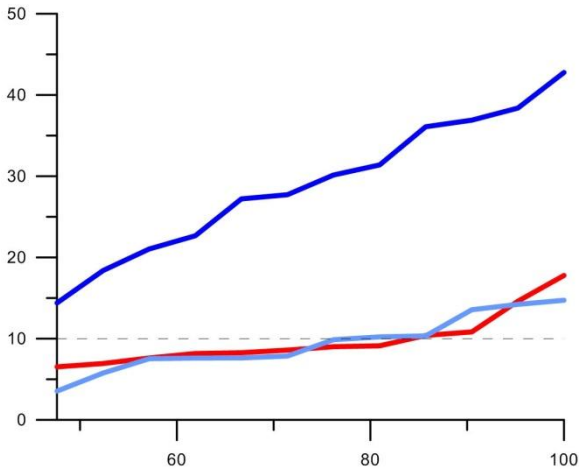

Figure 8: The relative mean speed prediction errors (y-axis) for the upper 50 pct of errors for horizontal measuring pairs with anemometer heights from 10-20m.The dark blue is the standard WAsP-IBZ, the light blue is WAsP-IBZ with ΔRIX correction with the constant *c* equal to 1.2 . The red curve shows the WAsP-CFD performance.

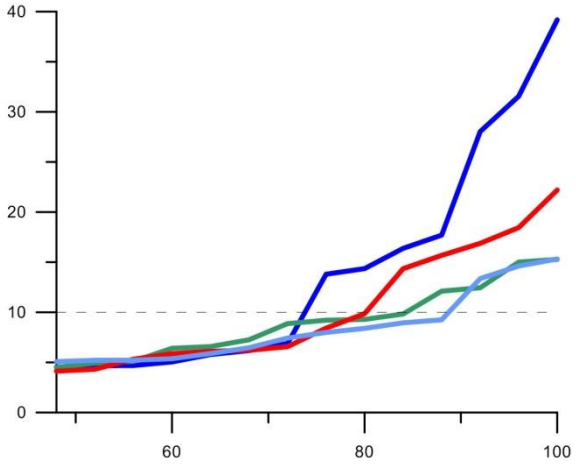

Figure 9: As figure 8, but for the 30-40m height range. The value for the constant in ΔRIX correction is again 1.2. Here we have added a green curve: IBZ modified setting a fixed “land-fill” slope of 0.125 (fitted to minimize error).

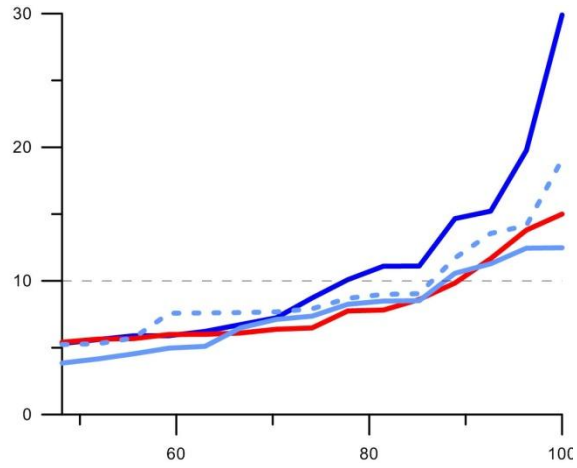

Figure 10: As figure 8, but for the 50-60m height range. The constant in the ΔRIX correction is here 0.8. The light blue dashed line corresponds to using the same constant (1.2) as for the lowest levels.

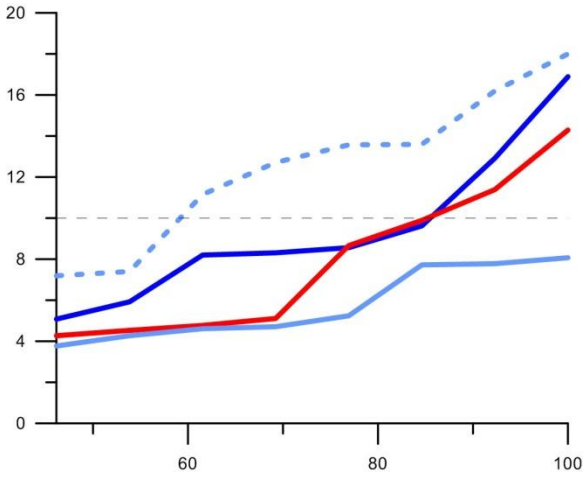

Figure 11: As figure 8, but for the 80-100m range. The constant in the ΔRIX correction is here 0.5. The light blue dashed line corresponds to using the same constant as for the lowest levels.

Figure 12 shows similarly the skill for the (total of 46) vertical pairs taking only the upward extrapolations (target anemometer above predictor on same met mast).

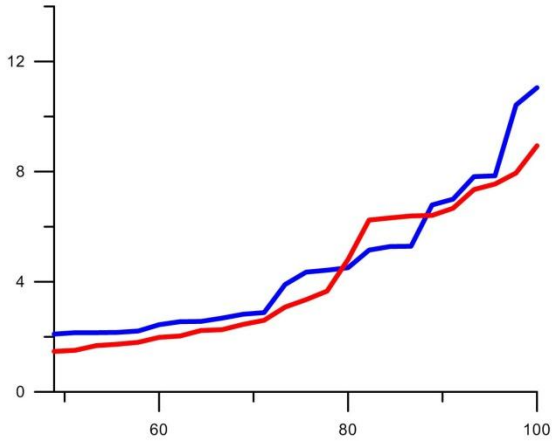

Figure 12: As figure 8, but for all upward extrapolations. For vertical extrapolations the ΔRIX correction is zero since ΔRIX=0.

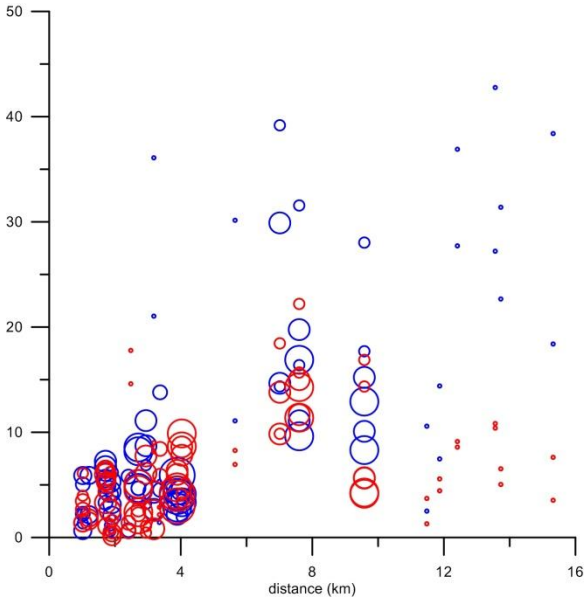

Figure 13: Bubble plot of the prediction error for WAsP-IBZ (blue) and WAsP-CFD (red) for horizontal extrapolations (data corresponding to those of the blue and red curves in figures 9-12). Percent error along the y-axis, mast horizontal distances in km along the x-axis. The bubble size is proportional to the height a.g.l.

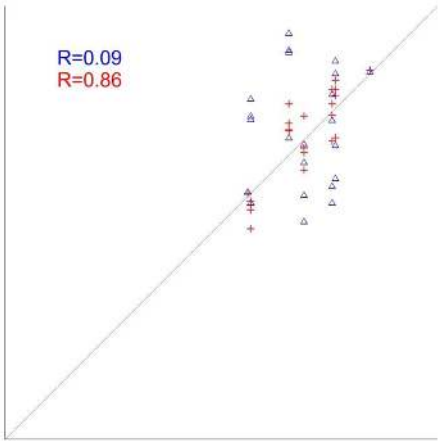

Figure 14: Scatter plot with correlation coefficients indicated for the 10-20m range. Blue is BZ, red is CFD, Predicted vs. observed wind speeds in arbitrary units.

Figure 14 shows the good correlation for the CFD for the 10-20m height range (almost entirely the 10m data from the RIX site [3]). The BZ shows zero correlation. These data includes the largest mast separations (figure 13, smallest bubbles); Figure 13 illustrates that over smaller distances the differences between BZ and CFD is much less. For the case of using the BZ modified with "land-fill" slope reduction, we find that if using the (low) value for the maximum slope of 0.125 rms errors and correlations at values comparable to those of CFD and the (calibrated) ΔRIX values could be obtained (figure 10). The last frame in figure 15 shows, however, the "cost" of this: Very strong, unrealistic smoothing of the smaller scales. The BZ-ΔRIX corrected field is practically indistinguishable from the uncorrected one because of the small variation of RIX over the area.

Figures 8-11 suggest that the BZ-ΔRIX method statistically is comparable in skill to CFD. However, one disturbing feature is the need for calibration of the constant *c* in the correction expression (section 2.1). Another, possibly more serious concern relates to the interpretation of the skill. For simplicity and sake of argument assume that the (known systematic) over prediction of orographic speed-up factors by the linear model(s) would tend to (statistically) follow something like:

$$F_{Linear} \sim F_{true}(1 + C \cdot RIX) ,$$

Where *C* is some constant. The argument being that choosing well exposed mast locations at high RIX sites (steep slopes) increases the chances that the linear model over predicts speed-up factors (consistent with the discussion in [3]) Since the prediction by WAsP of the mean speed at a target location "B" from the observations at location "A" is essentially:

$$u_m(B) \sim u_m(A) \cdot \frac{F_{linear}(B)}{F_{linear}(A)}$$

We find, by combining these expressions and expanding to first order that there will be a "spurious" correlation between the relative WAsP-BZ error and ΔRIX proportional to:

$$< error_B \cdot \Delta \mathrm{RIX}_{AB} > \sim$$

$$< \frac{u_A}{u_B} \frac{F_{true}(B)}{F_{true}(A)} C (\Delta RIX)^2 >$$

Here the <> denotes averaging over all AB pairs.This positive correlation stemming from BZ model deficiency and selective sampling, while statistically may allow a correction to lower rms errors, may incur an effective aliasing of the correction signal to larger scales than the smaller scale BZ error. We intend to look further into this in a more in-depth statistical analysis.

6 Discussion

The results show the expected superior performance of the fully dynamical CFD as compared to the linear BZ model.

The prediction errors may not solely be attributable to the flow models but may in part stem from anywhere in the data and model chain, including input wind data and site descriptions. The validation data is by no way ideal for an anywhere near thorough validation of the models as in particular the data are taken exclusively at well exposed hilltop and ridge sites.

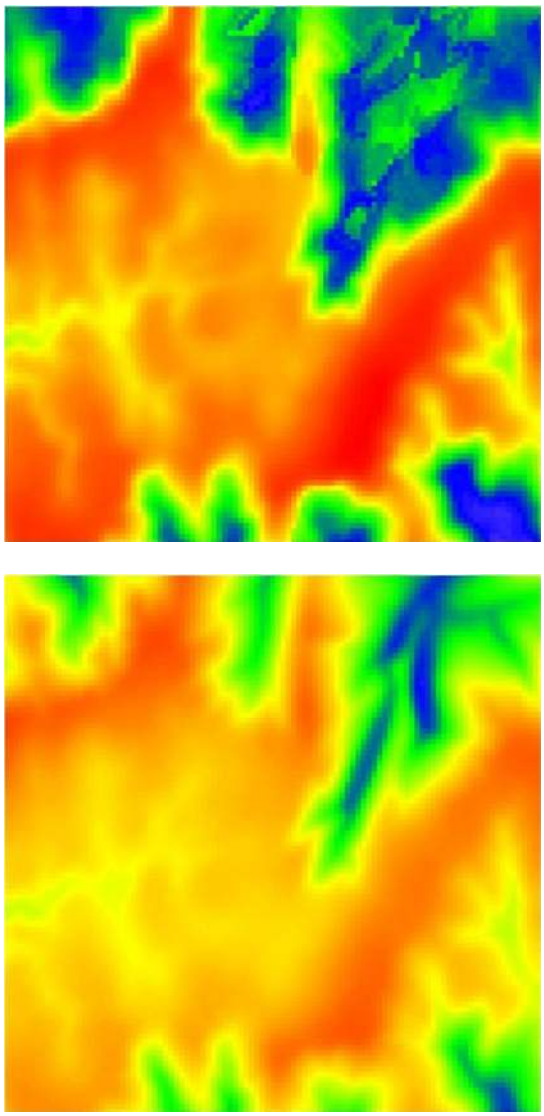

Figure 15: Top frame corresponds to the 2 by 2 km square in figure 8: CFD predicted mean speed field from 10m mast data at the center, but here for 40 a.g.l. The lower plot is the same area with the BZ predicted field. Values from blue to red; light green to reddest represent a factor 2.

The correction schemes considered (ΔRIX and landfill) as partial remedy against the shortcomings of the linear approach for these very complex sites should be expected to rely heavily on this particular nature of the available validation datasets. We see that the landfill method, while it may be useful as a minor

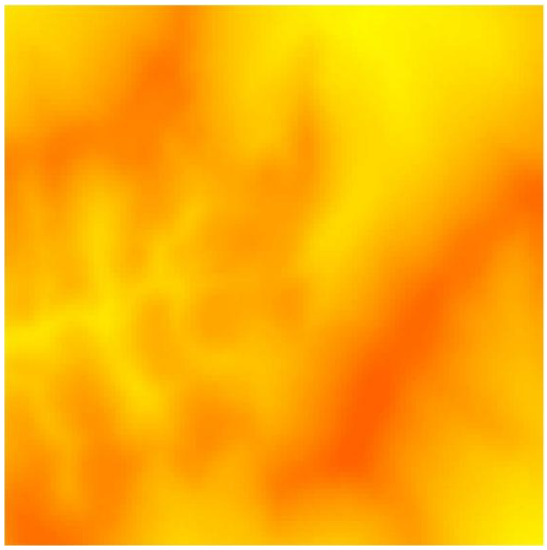

Figure 15 continued: The field predicted by BZ with the "land-fill" slope of 0.125 (as in figure 10). The excessive smoothing is evident.

modification, requires unrealistic low values of the landfill slope in order that rms errors become comparable to those of CFD .For more realistic landfill slopes the method may be useful, but the method needs refinement.

For the ΔRIX method this study supports the skill of the method to reduce WAsP-IBZ sample variance, and RIX as a useful complexity indicator. The correction method requires at least calibration in terms of height above ground. We could foresee a development of a simple formdrag model, that could make the method less empirical, and this could also benefit the CFD prediction accuracy by better specification of inflow conditions At the same time, however, the discussion in section 5 (and in [3]) indicate that it may be purely statistical, akin to a kind of spatial aliasing to erroneously propagate fine scale deficiencies in the linear model to larger scales. This needs further study.

In further model development and improvement it would be highly desirable to extend this analysis to many more complex sites with good quality data. Equally or more importantly large scale field experiments are needed in complex terrain

Acknowledgements

Thanks to Morten Thøgersen, EMD International A/S and Brian O. Hansen, DTU for obtaining datasets, and Lasse Svenningsen (EMD) for preparing and providing access to datasets and to Niels Gylling Mortensen and Ole Rathmann of DTU for providing additional datasets. Part of the work was performed under a grant from the Danish "Business Innovation Fund".

7 References

[1] Bechmann, A., J. Johansen and N.N. Sørensen, 2007. "The Bolund Experiment – Design of Measurement Campaign using CFD" Risø-R-1623(EN). ISBN 978-87-550-3638-3. Risø National Laboratory, Roskilde. 19pp.

[2] Troen, I. and E.L.Petersen, 1989. "European Wind Atlas", ISBN 87-550-1482-8, Risø National Laboratory, Roskilde. 656 pp.

[3] Bowen, A.J. and N.G. Mortensen, 2004. "WAsP prediction errors due to site orography." Risø-R-995(EN). Risø National Laboratory, Roskilde. 65 pp.

[4] Walmsley, J.L., I. Troen, D.P. Lalas and P. Mason, 1990, "Surface-layer flow in complex terrain: Comparison of models and full-scale observations." Boundary-Layer Meteorology **52**, 259-281.

[5] Hess, G.D. and J. L. Garratt, 2002, "Evaluating models of the neutral, barotropic planetary boundary layer using integral measures: Part 1. Overview.", Boundary-Layer Meteorology **104**, 333-358.

[6] Troen, I., 1990, "A high resolution model for flow in complex terrain." Proceedings of the AMS Ninth Symposium on Turbulence and Diffusion, Roskilde, Denmark, 417-420.

[7] Sempreviva, A.M., S.E. Larsen, N.G. Mortensen and I. Troen, 1990, "Response of neutral boundary layers to changes of roughness", Boundary-Layer Meteorology **50**, 205-225.

[8] Bechmann, A., N.N. Sørensen, J. Berg, J. Mann and P.E.Réthoré, 2011," The Bolund Experiment, Part II: Blind Comparison of Microscale Flow Models", Boundary-Layer Meteorology **141**, 245-271.

[9] Belcher, S.E., T.M. Newley and J.C.R. Hunt, 1993, "The drag on an undulating surface induced by the flow of a turbulent boundary layer.", J. Fluid. Mech. **,249**, 557-595.

[10] Wood, N. And P. J. Mason,1993, "The pressure force induced by neutral, turbulent flow over hills.", Q.J.R. Meteorol. Soc, **119**, 1233-1267.

[11] Taylor, P.A., R. I. Sykes and P. J. Mason, 1989, "On the parameterization of drag over small-scale topography in neutrally stratified boundary-layer flow", Boundary-Layer Meteorology **48**, 409-422.

[12] Bechmann, A., N.N. Sørensen, I. Troen, P-E Rethore, D. Cavar, A. Sogachev, I. Troen, M.C. Kelly, L-E Boudreault, E. Dellwik, 2014, "A Simple Guide to Microscale Terrain CFD", under preparation.

[13] Sørensen, N.N.,1995, "General Purpose Flow Solver Applied to Flow over Hills", PhD thesis, Risø-R-827 (EN).ISBN 87-550-2079-8. Risø National Laboratory, Roskilde. 154pp.

[14] Beljaars, A.C.M., A.R. Brown and N. Wood, 2004, "A new parametrization of orographic turbulent form drag", Q.J.R. Meteorol. Soc, **113**, 1327-1347.

[15] Michelsen J.A., 1994. "Basis3D – a platform for development of multiblock PDE solvers", Technical report AFM 92-05, Technical University of Denmark.

[16] Michelsen J.A., 1994. "Block structured multigrid solution of 2D and 3D elliptic PDE solvers", Technical report AFM 94-06, Technical University of Denmark.

[17] Launder B.E. and Spalding D.B., 1974. "The numerical computation of turbulent flows",Comput. Meths. Appl. Mech. Eng. 3(2), 269-289.